3-D Printed BCP Blocks with Different Pore Sizes for Regeneration in Rabbit Calvarial Defects

Young-Wook Seo (ywseo@yuhs.ac)
Yonsei University Dental Hospital
Jin-Young Park
Yonsei University Dental Hospital
Da-Na Lee
Yonsei University Dental Hospital
Xiang Jin
Yonsei University Dental Hospital
Jae-Kook Cha
Yonsei University Dental Hospital
Jeong-Won Paik
Yonsei University Dental Hospital
Seong-Ho Choi
Yonsei University Dental Hospital https://orcid.org/0000-0001-6704-6124

Research Article

Keywords: Animals, Bone regeneration, Different pore size, Hydroxyapatite-beta tricalcium phosphate,

Posted Date: March 15th, 2022

DOI: https://doi.org/10.21203/rs.3.rs-1437572/v1

Abstract

Background

Alveolar ridge augmentation is frequently performed in the deficient alveolar ridge to facilitate the placement of dental implants. Severe resorption of the bony ridge may occur because of aging or periodontal and periapical pathologies. When faced with this situation, a block bone graft might be indicated, since the block bone provides structural stability to the augmented site. The aim of this study was to compare three-dimensionally printed biphasic calcium phosphate (BCP) block bone substitutes with different pore sizes (0.8, 1.0 and 1.2 mm) for regeneration rabbit calvarial defects.

Material & Methods

Four circular defects were formed on the calvaria of ten rabbits. Each defect was randomly allocated to the following study groups: 1) Control group, 2) 0.8 mm group, 3) 1.0 mm group, and 4) 1.2 mm group. All specimens were harvested at 2 and 8 weeks postoperatively, and the samples were analyzed radiographically and histomorphometrically.

Results

Histologically, the BCP blocks remained unresorbed up to 8 weeks, and new bone formation occurred within the porous structure of the blocks. At the early healing period of 2 weeks, histomorphometric analysis revealed significantly greater new bone formation in the BCP groups compared to the control ($p < 0.05$). However, there were no significant differences between the groups with different pore sizes ($p > 0.05$). At 8 weeks, only the 1.0 mm group (3.42 ± 0.48 mm^2) showed a significantly greater area of new bone compared to the control group (2.26 ± 0.59 mm^2) ($p < 0.05$). Among the BCP block groups, 1.0 mm and 1.2 mm groups exhibited significantly greater area of new bone compared to the 0.8 mm group (3.42 ± 0.48 and 3.04 ± 0.66 vs 1.60 ± 0.70 mm^2, respectively).

Conclusions

Within the limitations of this study, 1.0 mm pore diameter of the BCP block bone substitute was the most optimal size for bone regeneration. The BCP block bone substitutes can be applied in bone defects for successful bone regeneration, and further study should be performed in more challenging defect configurations prior to the clinical application.

Introduction

Alveolar ridge augmentation is frequently performed in the deficient alveolar ridge to facilitate the placement of dental implants(1–3). Severe resorption of the bony ridge may occur because of aging or periodontal and periapical pathologies. When faced with this situation, a block bone graft might be indicated, since the block bone provides structural stability to the augmented site. Autogenous bone block has been considered as the gold standard due to the combined osteogenic, osteoinductive and osteoconductive properties. However, there are also disadvantages including additional surgical procedure for block harvesting, technical difficulty of the surgery, possible donor site morbidity and complications(4).

Thanks to the recent advances in digital dentistry and three-dimensional (3-D) printing technology, synthetic block bone substitutes can be customized to fit individual defect morphology. Among the various synthetic bone substitutes, biphasic calcium phosphate (BCP) – a combination of hydroxyapatite (HA) and beta-tricalcium phosphate (b-TCP), is the most frequently used(5). Calcium phosphate is the natural chemical constituent of the living bone; therefore, BCP has been known to exhibit excellent biocompatibility. The HA component provides the osteoconductive scaffold for cell migration, vascularization, and new bone formation (6–8) while b-TCP is more biodegradable and provides the source of calcium and phosphate ions for bone formation (5).

It is vital for the BCP block to contain interconnected pores, which allows cell infiltration and vascularization(9–13). The size of the pores can influence the rate of bone formation and material resorption. Previous studies have shown that larger pore sizes allow more rapid bone formation (14–16). This is because there is more space provided for initial bone formation, and greater surface area of the material is exposed to resorption by osteoclasts(5). However, it could be hypothesized that if the pore size exceeds a threshold, then the osteoconductivity of BCP will be outweighed by the ingrowth of fibrous tissues into the BCP block combined with the degradation of the biomaterial. Numerous studies have been performed to find the optimal pore size for bone formation, but results have been inconclusive(15–17).

In this study, the BCP block type substitutes with pore sizes of 0.8 mm, 1 mm, and 1.2 mm were fabricated by 3-D printing. Our hypothesis was that synthetic BCP block bone substitute with the largest pore size of 1.2 mm will facilitate the greatest amount of bone formation when placed in a bone defect. The aim of this study is to compare BCP blocks with different pore sizes for the regeneration of rabbit calvarial defects.

Material And Methods

2.1. Materials

3-D printed BCP blocks with varying pore sizes were used in this study. The BCP was composed of HA and b-TCP at the ratio of 60:40, and had pore sizes of 0.8, 1.0, and 1.2 mm respectively. A 3D-printed block bone substitute prepared by using a Digital Light Processing 3D printer (Cubicon Lux, Cubicon®,

Sungnam, Korea). This 3D printer had a resolution of 100 μm and can print layers with a 20–100 μm layer thickness. The manufacturing process was as follows(Fig. 1). Firstly, the bone substitute designs (Φ 8mm × 2mm) were converted into a stereolithography file that was used by the 3D printer to form the bone substitutes in a layer-by-layer manner. a ceramic slurry containing HA/b-TCP powder, acrylic monomer, dispersant, and photo-catalyst were prepared. Then, the UV light emitted from the projector was reflected by the mirror through the lens on to the ceramic slurry while it was being printed by the build plate. Thereafter, the residual monomers were completely removed through an in-furnace heat treatment (1250°C for 10 hours, Carbolite, Ubstadt-Weiher, Germany)(Fig. 2, Fig. 3).

2.2. Animals

Ten New Zealand White rabbits (12 weeks old and 2.8–3.2 kg in weight) were used in this experiment. Animals were housed in separate cages with standard laboratory conditions and diet. The animals had been given an acclimatization period of one week prior to the experiment. Housing protocol was according to the Association for Assessment and Accreditation of Laboratory Animal Care guidelines. All the procedures from animal selection, care, and preparation to anesthesia and surgical procedure followed the protocol approved by the Institutional Animal Care and Use Committee of Yonsei Medical Center, Seoul, Korea.

2.3. Study design

Four circular bone defects with a diameter of 8 mm were formed on the calvaria of 10 rabbits. Each defect was randomly allocated as follow: 1) Control group: empty, 2) 0.8 Group: BCP block group with 0.8mm pore size, 3) 1.0 Group: BCP block group with 1.0mm pore size, and 4) 1.2 Group: BCP block group with 1.2mm pore size (Fig. 4). All subjects in this study were sacrificed at 2 and 8 weeks after bone graft procedure, and micro-computed tomography (micro-CT) analysis, histomorphometric analysis and histological observation were performed on the experimental specimens.

2.4. Surgical procedure

A surgical procedure was performed based on the reference to the previously published studies(18, 19) (18, 19). General anesthesia was performed with isoflurane (2-2.5%) inhalation and alfaxan (5 mg/kg), medetomidine (0.25 mg/kg) intravenous injection. Oro-tracheal intubation was performed using size 6 tubes without ballooning for securing the airway. Disinfection of surgical site was done with povidone-iodine and local anesthesia was done with 2% lidocaine with 1:80,000 epinephrine injection. After making incision along the midline of the cranium, a full-thickness flap was elevated and the calvarium was exposed. Four circular defects with a diameter of 8 mm and a depth of 2 mm were created with a trephine bur without damaging underlying dura mater and cerebral tissue under copious saline irrigation. The defects on the calvarium were randomly assigned to one of the following four experimental groups; control group, 0.8mm group, 1.0mm group, and 1.2mm group. Each allocated defect was filled according to the study design. After the placement of materials, the flaps were carefully closed and sutured with the absorbable 4 – 0 suture material (Monosyn, B. Braun, Terrassa, Spain). General antibiotic therapy with enrofloxacin(10 mg / day) was given for 5 days after operation.

2.5. Analysis

Clinical observations

Any possible inflammatory signs and unexpected complications of the surgical site were observed on a daily basis until the sacrifice in 2 and 8 weeks after surgery. Any sign of infection, swelling, inflammation, wound dehiscence were not shown and no rabbit in this study was lost during the total experimental period.

Micro-CT analysis

The calvarial defect specimens (2weeks, 8weeks, 10 specimen each) were fixed with 10% formalin for 7 days and then scanned with micro-CT (SkyScan 1173, Bruker-micro CT, Kontich, Belgium) at a pixel size of 13.93 μm (130 kV, 60 μA). Scanned datasets were processed in digital imaging and communications in medicine (DICOM) format, and reconstructed with three dimensional (3D) reconstruction software (Nrecon reconstruction program [Ver 1.7.0.4], Bruker-CT, Kontich, Belgium).

The region of interest (ROI) for volume measurement in CT analysis were defined as follow:

- Superior border : the mucoperiosteal layer covering the defect.

- Lateral border : the margins of the original defect

- Inferior border : the dura meter

Radiopaque areas were distinguished from the total augmented area with 8-bit threshold grayscale values in a pixel size of 13.93 um. Grayscale value range from 50 to 255 were considered all mineralized tissue and between 50 to 90 were set for newly mineralized tissue in the defects. Above 90 of gray-scale value were indicated to be BCP material and under 50 of gray-scale value were fibro-vascular connective tissue. Within the ROI, the following volumes were measured using the software.

- Total Augmented Volume (TAV; $mm^{3)}$: Total volume including fibro-vascular connective tissue, newly formed bone, and grafted material volume within ROI.

- New Bone Volume (NBV; mm^3): Sum of Volume of newly formed bone volume in the defect

- Residual Material Volume (RMV; mm^3): residual grafted material volume in the defect.

The proportion of newly regenerated bone was calculated by the following formula.

Histomorphometric analysis

After sacrificing the rabbits of each experimental group, tissue fixation was performed in formalin solution at 4°C for one week. Before cutting each calvarial specimen, micro-CT was performed. Total 20

slides of tissue specimens were prepared by cutting the calvarial defect longitudinally. Hematoxylin-eosin is applied to un-decalcified, resin-embedded, bone sections to distinguish the mineralized bone matrix from osteoid.

At first, histologic slides were scanned with a digital slide scanner (Panoramic 250 FLASH III (3D HISTECH, Hungary). After the microscopic observation in entire slides including various tissues, the slide images were digitally captured. Slide image analysis program (Case Viewer 2.1; 3DHISTECH ltd., Budapest, Hungary) was used for histomorphometric analysis and the data measured from the scanned image were summarized in Excel.

The margin of ROIs was defined by the defect cut made by trephine bur. Superior border of the ROI was defined by the periosteum and the inferior border of the ROI was defined by the dura mater. Within the ROI, the following parameters were measured.

Within the ROI, the following areas were measured using the software.

- Total Augmented Area (TAA; $mm^{2)}$: Total area including fibro-vascular connective tissue, newly formed bone, and grafted material volume in the ROI.

- New Bone Area (NBA; mm^2): Sum of area of newly formed bone volume in the ROI.

- Residual Material Area (RMA; mm^2): residual grafted material area in the ROI.

Statistical analysis

For statistical analysis, SPSS software program (IBM SPSS Statistics 26, SPSS, Chicago, IL) was used. Total augmented bone volume, New bone volume, Residual material volume measurements from micro-CT by gray scale and Total augmented area, New bone area, Residual material area measurements from histomorphometric and histology were summarized by mean values and standard deviations. Kruskal-Wallis test and Mann-Whitney U test were used to analyze the statistic difference among the study groups at each time period(2,8 weeks) and between the same groups of different healing periods. $P < 0.05$ was considered as a statistical significance.

Result

Clinical observation

All experimental sites healed uneventfully, and were maintained without complications such as infection and wound dehiscence during the entire study period. At sacrifice, it could be seen that all of the BCP blocks remained within the grafted site.

Micro-CT volumetric analysis (Fig. 5, Fig. 6, Fig. 7, **Table 1)**

At 2 weeks, the BCP block groups exhibited a significantly greater NBV (mean [± SD] of 16.76 [± 3.36], 15.06 [± 2.77] and 16.02 [± 3.61] mm^3 for 0.8, 1.0 and 1.2 groups, respectively) compared to the control group (6.56 [± 3.53] mm^3) ($p < 0.05$) (Table 1). However, there were no significant differences between the BCP block groups. Regarding the TAV, all BCP block groups (161.86 [± 8.06], 177.21 [± 26.96], and 177.35 [± 18.40] mm^3 for 0.8, 1.0 and 1.2 groups, respectively) were significantly larger than the control group ($p < 0.05$). However, there was no significant difference between the BCP groups ($p > 0.05$). The 0.8 group showed a significantly greater RMV (67.89 [± 5.75] mm^3) compared to the 1.0 group (28.24 [± 3.65] mm^3) and 1.2 group (31.19 [± 1.24] mm^3) ($p < 0.05$).

At 8 weeks, the mean [± SD] NBV was the greatest in the 1.0 group (35.81 [± 5.73mm^3], followed by 1.2 group (34.10 [± 5.91] mm^3), 0.8 group (32.02 [± 3.41] mm^3), and the control group (24.11 [± 1.79] mm^3). All BCP block groups showed significantly greater NBV compared to the control group, however, there was no statistically significant difference between the BCP groups. There were no significant differences in TAV between the BCP groups. Only the 1.2 group and the 0.8 group (190.33 [± 16.60] mm^3 and 189.91 [± 24.60] mm^3, respectively) exhibited significantly greater TAV compared to the control group (151.68 [± 16.94] mm^3). The 0.8 group (70.53 [± 5.52] mm^3) exhibited significantly greater RMV compared to the 1.0 group (33.78 [± 2.68] mm^3) and 1.2 group (34.69 [± 3.09] mm^3).

When the 2- and 8-week groups were compared, all groups in the 8-week group had significantly greater NBV than their corresponding 2-week group. TAV showed no significant difference between 2 and 8 weeks.

Histomorphometric analysis (Fig. 8, Fig. 9, **Table 2)**

At 2 weeks, all BCP block groups exhibited significantly greater NBA (mean[± SD] of 0.30 [± 0.17], 0.38[± 0.38], 0.39[± 0.19] mm^2 for 0.8, 1.0 and 1.2 groups, respectively) compared to the control group (0.09[± 0.06]mm^2) ($p < 0.05$) (Table 2). However, there was no significant difference between the BCP groups. TAA was also significantly greater in all BCP block groups (15.74[± 1.95], 15.88[± 1.00], 16.83[± 1.24] mm^2 for 0.8, 1.0, 1.2 groups, respectively) compared to the control group (6.13[± 1.13] mm^2) ($p = 0.008 < 0.05$). RMA was greatest in the 0.8 group (9.61[± 2.14]mm^2), but there was no statistically significant difference.

At 8 weeks, only the 1.0 group (3.42[± 0.48]mm^2) showed a significantly greater NBA than the control group (2.26[± 0.59]) ($p = 0.03 < 0.05$). Between the BCP block groups, 1.0 and 1.2 groups exhibited significantly greater NBA compared to the 0.8 group. TAA was significantly larger in all BCP block groups (16.52[± 0.84], 15.85[± 1.04], 15.88[± 1.29] mm^2 for 0.8, 1.0, 1.2 groups, respectively) compared to the control group (5.78[± 1.10] mm^2) ($p < 0.05$). However, there was no significant difference between the BCP groups. In terms of the RMA, the 0.8 group (11.57[± 0.81]mm^2) was statistically significantly larger than the 1.0 group (5.24[± 0.14], $p = .0.016 < 0.05$) and 1.2 group (4.70[± 0.59], $p = 0.008 < 0.05$).

When the 2- and 8-week groups were compared, all groups in the 8-week group had significantly greater NBV than their corresponding 2-week group Compared with the 2-week groups, all BCP blocks at the 8-weeks showed a statistically significantly larger RMA ($p < 0.05$).

Histological observations

An example of histologic analysis results for each group at each time period was shown in Fig. 7.

Control group

At 2 weeks, the defect was partially filled with connective tissue and the center of the defect was sunk down with reduced total volume. New bone formation started from the adjacent native bone at the periphery of the defect.

At 8 weeks, none of the defects were fully filled with new bone, and some bony islands and bone bridge was observed.

0.8mm pore size group

At 2-weeks, the volume and shape of the defect were maintained by the BCP block and completely encapsulated with fibro-vascular tissue. The formation of new blood vessels for bone regeneration was observed and the initial bone regeneration started from periphery of the calvarial defect.

At 8-weeks, BCP block remained in place without notable degradation, new bone formation from the periphery to the center along the surface of the BCP block was observed. But the new bone did not merge with each other. In addition, new bone formation was observed in the pore area and mature bone was observed from the periphery of the defect. Overall, remarkable pattern of bone regeneration and growth was observed in the BCP block close to the dura meter.

1.0mm pore size group

At 2-weeks, the BCP block maintained the morphology of the formed defect, and an initial healing pattern was observed. Most of the interspaces between the BCP block lattice structure were filled with fibro-vascular tissue, but loosely structured tissue was observed in the center of the BCP block. A concave lower boundary due to the pressure of the brain tissue was observed on the dura meter contacted with the BCP block.

At 8 weeks, 1.0mm pore size group showed greatest new bone formation among the groups using the BCP block, and bone regeneration occurred on all surface of BCP block. A ring-shaped bone regeneration pattern surrounding the surface of BCP block was observed. In addition, the new bone was fused and matured with a pattern of connecting lattice structure of BCP block.

1.2mm pore size group

At 8-weeks, various types of bone growth were observed. Ring-shaped new bone regeneration surrounding the BCP block near to dura meter was observed. At the upper part of BCP block, osteogenesis with semi-lunar shape rather than ring shape was observed. However, fusion of regenerated bone was not observed, showing an independent bone regeneration pattern including independent island-shape bone formation

Discussion

Owing to the 3D-printing technology, synthetic block bone substitutes can be produced in customized shapes for application in bone augmentation procedures(8, 20–22). The optimal pore size within the bone blocks however, is yet to be established. The main outcomes of this study were: (1) the greatest new bone formation was achieved with the pore size of 1.0 mm, (2) the total augmented volume was maintained in all BCP block groups up to 8 weeks as were the volume of remaining materials, and (3) histologically, appositional new bone growth could be seen around the lattice structure of the BCP blocks, with almost full defect closure at 8 weeks.

The BCP block bone substitute in this study had a lattice structure composed of layers of parallel cylindrical rods constructed on top of each other in perpendicular arrangement. The pore size in this study referred to the uniform gap between the rods inside the lattice, and it could be observed that new bone was regenerated in this space(23, 24). A previous study suggested that the pore size of block bone substitute (hydroxyapatite scaffolds with small (90–120 mm) and large (350 mm) diameters) for enhancing vascularization and new bone formation should be larger than 300 μm(25–27), since pore sizes below 300 μm induced hypoxic conditions which suppressed direct bone regeneration(26, 28, 29). In agreement with this report, greater bone regeneration was achieved with the BCP block substitutes which have larger pore size of 500 μm in another study(15, 16). On the contrary, a previous study using pure b-TCP block substitute in the rabbit calvaria showed the greatest bone formation in the smallest pore size of 100 μm compared to 250 μm and 400 μm(17). However, this result might be explained by the greater biodegradability of b-TCP compared to HA. Considering the lower biodegradability of HA compared to b-TCP, greater pore size is needed with higher ratio of HA in the mixture of biomaterials(20–22). Using the 60:40 ratio of HA to b-TCP in this study, the greatest new bone formation was achieved with the pore size of 1.0 mm after 8 weeks of healing.

An ideal BCP block would maintain the space of the defect until the defect has been fully regenerated. The remaining material can be biodegraded and become replaced by new bone, as long as there is sufficient new bone to facilitate the placement of dental implants(30, 31). The most suitable rate of degradation may vary according to the size, configuration of the bone defect and the individual healing ability of the patient(12, 13). Nonetheless, the ultimate purpose of designing the most ideal block structure with adequate pore size would be to accelerate the bone regeneration process. As shown by the results of this study, the BCP bone substitute was unresorbed during the 8 weeks of healing period regardless of the pore size, indicated by the maintenance of total augmented volume as well as the remaining material. Therefore, using this biomaterial, it would be reasonable to assume that greater pore size would allow greater bone formation. On the other hand, as the pore size increases, the density of the

lattice structure would decrease and the compression strength would also decrease consequently(32). It has been shown previously that compression strength, chemical stability, and cytotoxicity of BCP blocks with pore sizes of 0.8 mm to 1.4 mm were reported, which accelerated bone regeneration without unwanted deformation or destruction of the BCP blocks(14). The BCP block used in this study promoted bone regeneration without infection or unwanted complications, and showed excellent biocompatibility, biodegradability, osteo-inductivity, and osteo-conductivity. Therefore, predictable results can be obtained by applying the customized BCP block using 3-D printing to the challenging procedure for reconstruction of a wide range of complex bone defects.

In the histological analysis of this study, new bone was regenerated along the lattice structure in a BCP block with a pore size of 1.0 mm, and osseointegration fused between the new bones, showing accelerated bone regeneration. However, in the 1.2 mm pore size, bone regeneration occurred with ring shape on BCP surface of surrounding lattice structure, but the connection (fusion) between new bones did not appear and bone regeneration was separately growth. These results showed different results from the results of previous studies that the larger pore size between the lattice structures, the better the initial bone regeneration(14), and the critical pore size of the BCP block is thought to exist between 0.8mm and 1.2mm. As in this study, when the pore size becomes larger than the critical size, the fibrous tissue over the defect penetrates and bone regeneration does not occur(27, 29). Therefore, further studies will be needed to prevent unwanted fibrotic tissue involvement using optimal membranes.

In addition, synthetic BCP blocks are based on HA and beta-TCP that may enhance greater new bone regeneration rate in physiological conditions. As can be seen from the results of RMV (RMA) in this study, it showed the result of maintaining the volume during a sufficient healing period and increasing the new bone synthesis. In addition, it will be possible to obtain predictable results by increasing suitability and initial stability in the challenging GBR procedure in the destroyed ridge defect by using the synthetic bone that can be customized by 3-D printing. In addition, compared to the particle type, block type graft could reduce surgical time, the risk of postoperative complication including infection, swelling and patient's morbidity.

In this study, to compare bone regeneration according to the pore size itself, a simple bone graft procedure was used rather than GBR (guided bone regeneration) which using a covering membrane. In the previous systematic review and meta-analysis, it was found that GBR technique using a bone graft material and membrane was more effective for bone regeneration than bone grafting using only a bone graft material(33). These studies mainly analyzed particle-type bone graft materials, and studies using block-type bone graft materials are still insufficient. Therefore, in future studies, it will be necessary to study optimal bone regeneration using a combination of various membranes.

Conclusion

In conclusion, within the limitation of this study, the 3-D printed BCP block with a medium pore size (1.0 pore size, 68% porosity rate) showed greatest new bone regeneration at 8weeks compared to other pore

size groups. And the use of the BCP block substitutes promoted faster bone regeneration than the control group. In addition, the BCP blocks maintained volume and space for bone regeneration in sufficient healing period(8weeks) and showed greater osteo-conductivity and bio-compatibility without any complication. Further studies are needed to investigate the optimal combination with various membranes combined with BCP substitutes and three-dimensional structure for faster bone regeneration.

Declarations

Ethics approval and consent to participate

Not applicable

Consent for publication

Not applicable

Availability of data and materials

All data generated or analyzed during this study are included in this published article.

Competing interests

The authors declare that they have no competing interests.

Funding

This study was supported by the National Research Foundation of Korea (NRF) grant funded by the Korea government (Ministry of Science, ICT & Future Planning) (No. NRF-2017R1A2B4002782).

Authors' contributions

S.-H.C. conceived the ideas, and reviewed/revised the manuscript; Y.-W.S.and J.-Y.P. collected and analyzed the data and drafted the manuscript; Y.-W.S., D.-N.L., and X.J. performedthe animal experiments; and Dentium®, Suwon, Korea manufactured the materials; S.-H.C., J.-Y.P., J.-K.C., and J.-W.P. critically reviewed and revised the manuscript. All authors have read and agreed to the published version of the manuscript.

Acknowledgements

This study was supported by the National Research Foundation of Korea (NRF) grant funded by the Korea government (Ministry of Science, ICT & Future Planning) (No. NRF-2017R1A2B4002782).

References

1. Lee JS, Cha JK, Kim CS. Alveolar ridge regeneration of damaged extraction sockets using deproteinized porcine versus bovine bone minerals: A randomized clinical trial. Clin Implant Dent Relat Res. 2018;20(5):729-37.
2. Chavda S, Levin L. Human Studies of Vertical and Horizontal Alveolar Ridge Augmentation Comparing Different Types of Bone Graft Materials: A Systematic Review. J Oral Implantol. 2018;44(1):74-84.
3. Barone A, Aldini NN, Fini M, Giardino R, Calvo Guirado JL, Covani U. Xenograft versus extraction alone for ridge preservation after tooth removal: a clinical and histomorphometric study. J Periodontol. 2008;79(8):1370-7.
4. Roccuzzo M, Ramieri G, Bunino M, Berrone S. Autogenous bone graft alone or associated with titanium mesh for vertical alveolar ridge augmentation: a controlled clinical trial. Clin Oral Implants Res. 2007;18(3):286-94.
5. Kato E, Lemler J, Sakurai K, Yamada M. Biodegradation property of beta-tricalcium phosphate-collagen composite in accordance with bone formation: a comparative study with Bio-Oss Collagen® in a rat critical-size defect model. Clin Implant Dent Relat Res. 2014;16(2):202-11.
6. De Oliveira JF, De Aguiar PF, Rossi AM, Soares GA. Effect of process parameters on the characteristics of porous calcium phosphate ceramics for bone tissue scaffolds. Artif Organs. 2003;27(5):406-11.
7. Ramesh N, Moratti SC, Dias GJ. Hydroxyapatite-polymer biocomposites for bone regeneration: A review of current trends. J Biomed Mater Res B Appl Biomater. 2018;106(5):2046-57.
8. Hwang JW, Park JS, Lee JS, Jung UW, Kim CS, Cho KS, et al. Comparative evaluation of three calcium phosphate synthetic block bone graft materials for bone regeneration in rabbit calvaria. J Biomed Mater Res B Appl Biomater. 2012;100(8):2044-52.
9. Roosa SM, Kemppainen JM, Moffitt EN, Krebsbach PH, Hollister SJ. The pore size of polycaprolactone scaffolds has limited influence on bone regeneration in an in vivo model. J Biomed Mater Res A. 2010;92(1):359-68.
10. Cheng MQ, Wahafu T, Jiang GF, Liu W, Qiao YQ, Peng XC, et al. A novel open-porous magnesium scaffold with controllable microstructures and properties for bone regeneration. Sci Rep. 2016;6:24134.
11. Lim TC, Chian KS, Leong KF. Cryogenic prototyping of chitosan scaffolds with controlled micro and macro architecture and their effect on in vivo neo-vascularization and cellular infiltration. J Biomed Mater Res A. 2010;94(4):1303-11.
12. Hing KA. Bone repair in the twenty-first century: biology, chemistry or engineering? Philos Trans A Math Phys Eng Sci. 2004;362(1825):2821-50.
13. Hing KA. Bioceramic bone graft substitutes: influence of porosity and chemistry. International journal of applied ceramic technology. 2005;2(3):184-99.
14. Lim HK, Hong SJ, Byeon SJ, Chung SM, On SW, Yang BE, et al. 3D-Printed Ceramic Bone Scaffolds with Variable Pore Architectures. Int J Mol Sci. 2020;21(18).

15. Chang BS, Lee CK, Hong KS, Youn HJ, Ryu HS, Chung SS, et al. Osteoconduction at porous hydroxyapatite with various pore configurations. Biomaterials. 2000;21(12):1291-8.
16. Gauthier O, Bouler JM, Aguado E, Pilet P, Daculsi G. Macroporous biphasic calcium phosphate ceramics: influence of macropore diameter and macroporosity percentage on bone ingrowth. Biomaterials. 1998;19(1-3):133-9.
17. Diao J, OuYang J, Deng T, Liu X, Feng Y, Zhao N, et al. 3D-Plotted Beta-Tricalcium Phosphate Scaffolds with Smaller Pore Sizes Improve In Vivo Bone Regeneration and Biomechanical Properties in a Critical-Sized Calvarial Defect Rat Model. Adv Healthc Mater. 2018;7(17):e1800441.
18. Kitayama S, Wong LO, Ma L, Hao J, Kasugai S, Lang NP, et al. Regeneration of rabbit calvarial defects using biphasic calcium phosphate and a strontium hydroxyapatite-containing collagen membrane. Clin Oral Implants Res. 2016;27(12):e206-e14.
19. Pae HC, Kang JH, Cha JK, Lee JS, Paik JW, Jung UW, et al. 3D-printed polycaprolactone scaffold mixed with beta-tricalcium phosphate as a bone regenerative material in rabbit calvarial defects. J Biomed Mater Res B Appl Biomater. 2018;0(0).
20. Sohn JY, Park JC, Um YJ, Jung UW, Kim CS, Cho KS, et al. Spontaneous healing capacity of rabbit cranial defects of various sizes. J Periodontal Implant Sci. 2010;40(4):180-7.
21. Pae HC, Kang JH, Cha JK, Lee JS, Paik JW, Jung UW, et al. 3D-printed polycaprolactone scaffold mixed with β-tricalcium phosphate as a bone regenerative material in rabbit calvarial defects. J Biomed Mater Res B Appl Biomater. 2019;107(4):1254-63.
22. Pae HC, Kang JH, Cha JK, Lee JS, Paik JW, Jung UW, et al. Bone regeneration using three-dimensional hexahedron channel structured BCP block in rabbit calvarial defects. J Biomed Mater Res B Appl Biomater. 2019;107(7):2254-62.
23. Rh Owen G, Dard M, Larjava H. Hydoxyapatite/beta-tricalcium phosphate biphasic ceramics as regenerative material for the repair of complex bone defects. J Biomed Mater Res B Appl Biomater. 2018;106(6):2493-512.
24. Tarafder S, Bose S. Polycaprolactone-coated 3D printed tricalcium phosphate scaffolds for bone tissue engineering: in vitro alendronate release behavior and local delivery effect on in vivo osteogenesis. ACS Appl Mater Interfaces. 2014;6(13):9955-65.
25. Karageorgiou V, Kaplan D. Porosity of 3D biomaterial scaffolds and osteogenesis. Biomaterials. 2005;26(27):5474-91.
26. Kuboki Y, Jin Q, Takita H. Geometry of carriers controlling phenotypic expression in BMP-induced osteogenesis and chondrogenesis. J Bone Joint Surg Am. 2001;83-A Suppl 1(Pt 2):S105-15.
27. Tsuruga E, Takita H, Itoh H, Wakisaka Y, Kuboki Y. Pore size of porous hydroxyapatite as the cell-substratum controls BMP-induced osteogenesis. J Biochem. 1997;121(2):317-24.
28. Jin QM, Takita H, Kohgo T, Atsumi K, Itoh H, Kuboki Y. Effects of geometry of hydroxyapatite as a cell substratum in BMP-induced ectopic bone formation. J Biomed Mater Res. 2000;51(3):491-9.
29. Kuboki Y, Jin Q, Kikuchi M, Mamood J, Takita H. Geometry of artificial ECM: sizes of pores controlling phenotype expression in BMP-induced osteogenesis and chondrogenesis. Connect Tissue Res.

2002;43(2-3):529-34.
30. Hulbert SF, Young FA, Mathews RS, Klawitter JJ, Talbert CD, Stelling FH. Potential of ceramic materials as permanently implantable skeletal prostheses. J Biomed Mater Res. 1970;4(3):433-56.
31. Wang HL, Boyapati L. "PASS" principles for predictable bone regeneration. Implant Dent. 2006;15(1):8-17.
32. Tarafder S, Dernell WS, Bandyopadhyay A, Bose S. SrO- and MgO-doped microwave sintered 3D printed tricalcium phosphate scaffolds: mechanical properties and in vivo osteogenesis in a rabbit model. J Biomed Mater Res B Appl Biomater. 2015;103(3):679-90.
33. Urban IA, Montero E, Monje A, Sanz-Sánchez I. Effectiveness of vertical ridge augmentation interventions: A systematic review and meta-analysis. J Clin Periodontol. 2019;46 Suppl 21:319-39.

Tables

Table 1. The results from micro-CT analysis.
****Values are presented as mean [± standard deviation] (mm^3)**
TAV : Total augmented volume, NBV : New bone volume, RMV : Residual material volume
[a] Statistically significant difference compared to the control group.;
[b] Statistically significant difference compared to the 0.8mm group.
[c] Statistically significant difference compared to the corresponding 2-week group at 2 weeks.

Healing period	Group	TAV	NBV	RMV
2 weeks (n=5)	Control	132.28 [±12.29]	6.56 [±3.53]	-
	0.8 mm	161.86 [±8.06][a]	16.76 [±3.36][a]	67.89 [±5.75]
	1.0 mm	177.21 [±26.96][a]	15.06 [±2.77][a]	28.24 [±3.65][b]
	1.2 mm	177.35 [±18.40][a]	16.02 [±3.61][a]	31.19 [±1.24][b]
8 weeks (n=5)	Control	151.68 [±16.94]	24.11 [±1.79][c]	-
	0.8 mm	189.91 [±24.60][a]	32.02 [±3.41][a],[c]	70.53 [±5.52]
	1.0 mm	170.93 [±16.61]	35.81 [±5.73][a],[c]	33.78 [±2.68][b],[c]
	1.2 mm	190.33 [±16.60][a]	34.10 [±5.92][a],[c]	34.69 [±3.09][b],[c]

Table 2. The results from histomorphometric analysis.
**Values are presented as mean [± standard deviation] (mm^2)
TAA : Total augmented area, NBA : New bone area, RMA : Residual material area.
[a] Significantly greater than the control group;.
[b] Significantly greater compared to the 0.8 group.
[c] Significantly greater compared to the corresponding 2-week group.

Healing period	Group	TAA	NBA	RMA
2weeks (n=5)	Control	6.13±1.13	0.09±0.06	-
	0.8 mm	15.74±1.95[a]	0.30±0.17[a]	9.62±2.13
	1.0 mm	15.88±1.00[a]	0.38±0.38[a]	5.15±1.19
	1.2 mm	16.83±1.24[a]	0.39±0.19[a]	5.51±0.59
8weeks (n=5)	Control	5.78±1.10	2.26±0.59[c]	-
	0.8 mm	16.52±0.84[a]	1.60±0.70[c]	11.57±0.81
	1.0 mm	15.85±1.04[a]	3.42±0.48[a],[b], [c]	5.24±0.14[b]
	1.2 mm	15.88±1.29[a]	3.04±0.66[b], [c]	4.70±0.59[b]

Figures

Figure 1 : BCP block manufacturing procedure by DLP(Digital light processing)

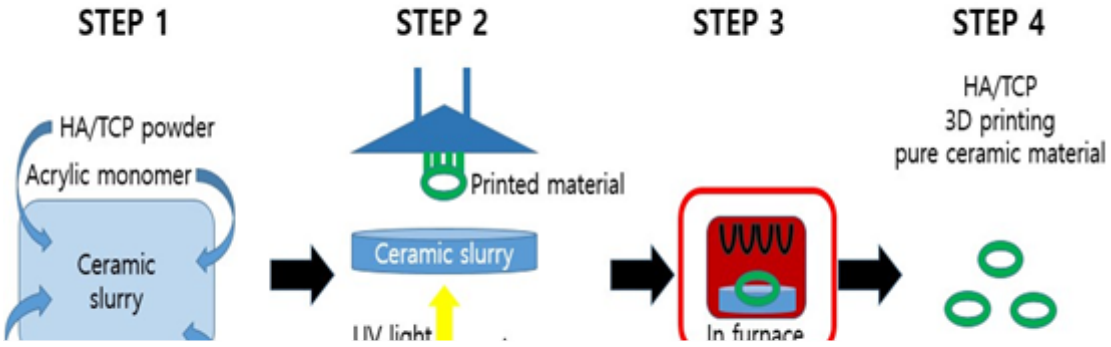

Figure 1

See image above for figure legend.

Figure 2 : structural design of BCP of 0.8mm(porosity rate 62%), 1.0mm(porosity rate 68%), 1.2mm(porosity rate 77%) (from left to right)

Figure 2

See image above for figure legend.

Figure 3 : microstructural feature of 3-D printed BCP bone substitutes (SEM, 3.0kV 30x, 100x, 300x, 1,000x, 3,000x). All SEM images showed pure BCP block (HA-b-TCP) without residual polymers.

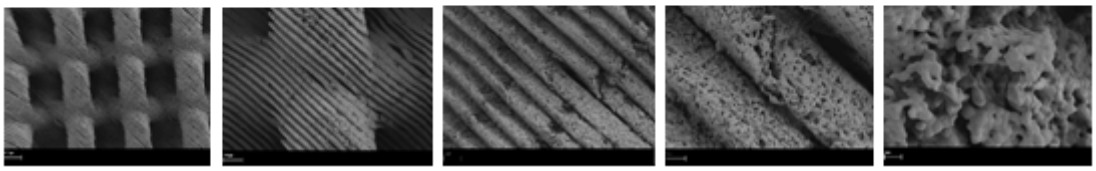

Figure 3

See image above for figure legend.

Fig. 4. Figure 4 :study design for rabbit calvarial defect model. (A) 4 circular defects preparation using 8mm in diameter, 2mm depth surgical trephine bur. (B) Each defect was randomly chosen for bone graft.
Clock wise from upper left; control group, 0.8mm pore size group, 1,0mm pore size group, and 1.2mm pore size group

Figure 4

See image above for figure legend.

Figure 5 : Reconstructed image of micro-CT views at 2weeks and, 8 weeks.
Left: 2weeks (control, 0.8, 1.0, 1.2, clockwise from upper left),
Right: 8weeks (control, 0.8, 1.0, 1.2, clockwise from upper left)

Figure 5

See image above for figure legend.

Figure 6: Micro-CT analysis on 2weeks, 8weeks group of healing period. At 2 weeks in the control group, the defects were rarely filled, and even at 8 weeks, the defects were partially filled with a thin new bone bridge.

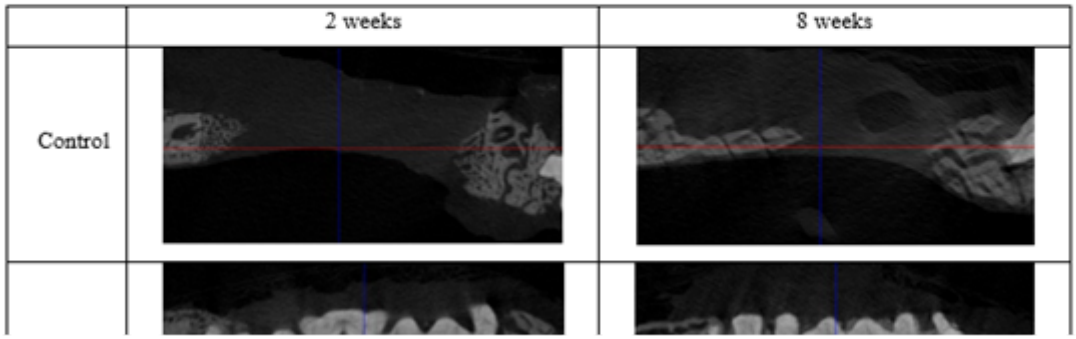

Figure 6

See image above for figure legend.

Figure 7. comparison of new bone volume by micro-CT analysis

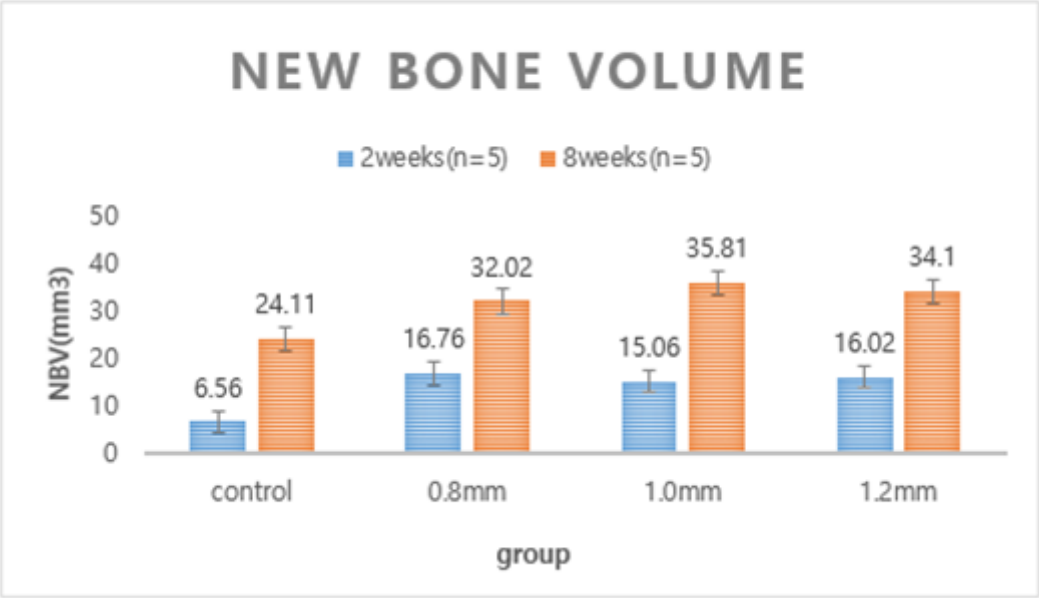

Figure 7

See image above for figure legend.

Figure 8

See image above for figure legend.

Figure 9

See image above for figure legend.